Multifunctional Bio-Nano Patterns Derived from Colloidal Self-Assembly as Model Surfaces to Study Antigen-Antibody Interactions

S. Krishnamoorthy, J. P. Wright, O. Worsfold, T. Fujii, M. Himmelhaus*

Fujirebio, Inc., Frontier Research Department, Bionanotechnology Research Project, 51 Komiya-cho, Hachioji-shi 192-031, Japan, ml-himmelhaus@fujirebio.co.jp

ABSTRACT

This paper presents a simple and effective way of preparing nanopatterns made of organic self-assembled monolayers on large surface areas by means of nanosphere lithography and exploring the capability of these patterns for immobilization of antibodies. The large pattern size allows for a detailed surface analysis via infrared spectroscopy and X-ray photoelectron spectroscopy, thereby revealing quality of the chemical patterns as well as allowing precise determination of the overall surface fraction of the functionalized patches. In a second step, the patterns are used for an in-situ surface plasmon resonance study on the physisorption of antibodies, followed by specific binding of antigens.

Keywords: nanosphere lithography, nanopatterning, biosensing, surface plasmon resonance, antigen-antibody interaction

1 INTRODUCTION

One of the key targets in the further development of label-free techniques utilized for biosensing is the optimization of the activity of the biological probe used for targeting the wanted analyte. This is a major issue, because most techniques rely on immobilization of the probe onto a surface interfacing between the specific recognition event and a physical transducer mechanism. This surface confinement of the probe, however, restricts its activity as compared to its native state in liquid due to a number of constraints, like reduced accessibility, steric hindrance, and probe-surface interactions causing degeneration or the blocking of active sites.[1] Therefore, strategies for immobilization of probes in a close to natural state have been explored intensively during the last decade.[2] Besides various attempts for oriented probe adsorption that assures an optimum orientation of the active site with respect to the confining surface, nanopatterning could contribute to increase in accessibility and function of the probe by suitable tailoring its immediate environment. Such tailoring could prove promising when the produced patterns are of the dimensions of the order of the probe, thereby allowing for fine adjustments of structure and topography on the relevant scale.

Despite its importance, the investigation of the effect of nanopatterning on probe activity is not a straightforward task. Direct comparison of the nanopatterned substrates with non-patterned counterparts using the existing biosensing techniques requires that the nanopatterns are spread over a large area with reasonable homogeneity and integrity. This would enable their study using state-of-the-art systems with sensing areas typically in the range from several hundred microns to several millimeters. Microscopic techniques, such as scanning probe microscopy, which provides lateral resolution on the required nanometric scale - unless carried out under liquid - mainly speak of the mechanical properties of the surface-bound species, such as the topography and elasticity. Accordingly, information on structure and state of the immobilized biomolecules is difficult to extract from such data.

We therefore explore the potential of large-scale nanopatterns, which can be analyzed with surface analytical tools that yield averaged information from a large areas of the surface. For this purpose, we utilize nanosphere lithography (NSL), which has become a popular tool as a patterning technique recently because the method is cheap and involves extremely simple procedures compared with other nanopatterning techniques, such as electron-beam lithography or scanning probe-related nanolithography. NSL can also be applied to a wide range of organic and inorganic materials. If combined with selective deposition of organic self-assembled monolayers (SAMs), NSL provides a feasible tool for the bio-functionalization of substrates to create next-generation biosensors or other bio-mimetic devices.

In this article, we explore the potential of NSL towards the fabrication of large-scale nanopatterns of antibodies embedded in a protein-resistant matrix and demonstrate the quality of the patterns formed through highly sensitive surface analysis tools, such as surface plasmon resonance (SPR), infrared reflection absorption spectroscopy (IRRAS), and X-ray photoelectron spectroscopy (XPS). Atomic force microscopy (AFM) is further used to verify the findings on microscopic scale.

As we will show in what follows, the produced nanopatterns typically cover only about 10% of the total surface area, thus emphasizing the demand for proper

surface passivation with respect to non-specific adsorption of biomolecules on the embedding matrix. Absence of an efficient non-fouling matrix can result in significant non-specific protein adsorption to the surface due to the hydrophobic effect, an aspect that has not been addressed in earlier work by other authors.[3]

2 EXPERIMENTAL

2.1 Preparation of Chemical Nanopatterns

To obtain large-scale nanopatterns of high homogeneity even in the cm^2 regime, polystyrene (PS) beads of 500 nm nominal diameter were adsorbed onto a gold surface coated with mercaptohexadecanoic acid (MHD) via carbodiimide-mediated adsorption. [4] This procedure yields random-close-packed particle layers with a surface coverage of 54.7% with high reproducibility, which is crucial for our work. After depositing the colloidal mask, the non-masked MHD is removed from the gold surface by means of reactive ion etching (RIE) in an oxygen plasma (SAMCO, Ltd., at 10sccm, 10Pa, 20W, 60s). Then, the mask is removed by means of a chloroform treatment, and the sample is subsequently immersed into an ethanolic solution of mercapto-polyethyleneglycol (PEG). Depending on the purpose (surface characterization or biomolecular adsorption studies via SPR), either silicon (100) wafers or glass cover slips (Biacore) were used as substrates. The overall procedure for fabricating the nanopatterns is sketched in Figure 1.

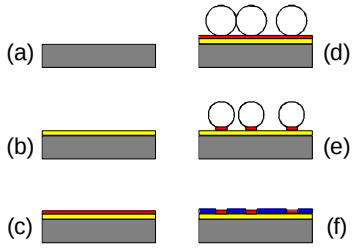

Figure 1: Preparation of homogeneous large-scale nanopatterns. A silicon or glass substrate (a) is coated with a 30-50 nm thick gold film using Cr as adhesion promoter (b). The gold is chemically functionalized by means of MHD (c), then the colloidal mask is deposited as described in the literature (d).[4] The colloidal beads form contact points of about 200 nm in diameter with the MHD-coated substrate. The non-covered MHD is removed from the gold surface by means of RIE (e). Finally the colloidal mask is removed and the free gold area is coated with PEG-SH SAM for introduction of a protein-resistant matrix.

2.2 Characterization of Nanopatterns

The resulting nanopatterns were analyzed by a number of surface-analytical methods to assure proper coating and for precise determination of the ratio between functional surface area and protein-resistant matrix.

IRRA spectra were obtained by means of a JEOL FTIR 680 plus spectrometer, equipped with a high angle reflection unit (80° incidence) and a dry-air purge system. Samples were referenced against a gold substrate of same origin, however coated with a perdeuterated alkanethiol.

XP spectra were acquired with a JEOL SP-9200 surface analysis system at a base pressure of $4x10^{-7}$torr. The non-monochromatic MgKα source was operated at 100W emission power. The hemispherical electron analyzer was set to a pass energy of 50eV for wide, and 10eV for detailed scans. The system was operated in macroscopic detection mode with a footprint of the electron analyzer entrance aperture on the sample surface of about 3mm diameter.

Scanning probe images were acquired with a Digital Instruments Dimension 3100 using ultrasharp silicon nitride coated Si cantilevers with a force constant of 0.12N/m from Mikromasch, Estonia.

2.3 In-situ Antigen/Antibody Adsorption

The kinetics of antibody (Ab) adsorption onto the patterned substrates and subsequent binding of the antigen (Ag) was monitored in-situ by means of a Biacore X SPR system. Phosphate Buffered Saline (PBS) solution at pH 7.2 was used as the running buffer. The samples were prepared in the same buffer, and were injected after ensuring a stable flow of the running buffer. Flow rates of 5µl/min, and 35µl sample quantity were used each time, and the experiments were carried out at 25°C. The experiments were performed on Biacore chips consisting of SAMs of PEG, MHD and PEG/MHD patterns. SPR response of the following three consequent pulses was monitored: 1. 37µg/mL solution of anti-mouse IgG, 2. BSA, 1%, and 3. antigen to α-feto protein at 50µg/mL concentration. The results are presented in Figure 5.

3 RESULTS AND DISCUSSION

For visualization of the fabricated nanopatterns, Figure 2 displays AFM friction force images of the patterns obtained after RIE treatment of the MHD-coated gold surfaces and subsequent bead removal. The contrast between MHD islands and gold surface is good enough to identify the spots of the formerly positioned PS beads clearly. Figure 2 shows patterns achieved after 15s (Fig. 2a) 30s (Fig. 2b) and 60s (Fig. 2c) of RIE treatment. After 15s of etching, the MHD patches are still interconnected, causing a poorly defined pattern, while 30 and 60s exposures yield well separated spherical patches of MHD SAMs. We found the patterns obtained after 60s treatment most suitable for further experiments. The diameter of the MHD patches obtained in this case was 200nm. The maximum coverage of the surface with these patches is obtained if the colloidal mask deposited achieves the jamming limit of random sequential adsorption. In this case, 54.7% of the surface is covered with beads of 500nm in diameter. Since we reduce the size of the patches to 200nm via RIE, the resulting maximum surface coverage is given by $\chi_{max} = 0.547 \times (200/500)^2 = 8.8\%$.

In a subsequent step, the clean gold is filled with PEG to render the surface protein-resistant except for the MHD-coated patches. This treatment is of utmost importance to avoid any misinterpretation of the influence of patterning on the activity of the adsorbed antibodies due to unwanted interaction with the non-functionalized area, in particular because this area occupies over 90% of the surface. We performed therefore an extensive surface analysis of the resulting patterns by means of IRRAS and XPS to prove their proper formation.

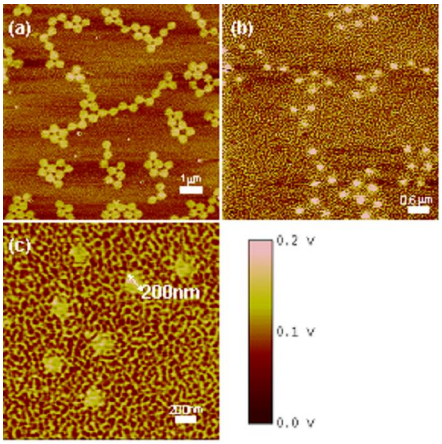

Figure 2: AFM friction force images of MHD patterns formed on a clean gold surface after RIE and subsequent removal of the colloidal mask. (a) pattern formed from 500nm colloidal beads after 15s RIE; (b) after 30s; (c) after 60s.

Figure 3 shows IRRAS spectra of the C-O-C stretching vibration region, which is of importance for the interpretation of the structure of the PEG layer. As has been demonstrated for similar PEG systems,[5] the resonance at 1119cm^{-1} can be assigned to a stretching vibration with a transition dipole moment along the main axis of the molecule, while that at 1147cm^{-1} is oriented perpendicular to that axis. Therefore, the intensity ratio of these two modes can be used to decide whether the PEG forms coils or brushes on the surface. Obviously, both the homogeneous PEG film that serves as reference and the film formed on a previously coated MHD layer after 60s of RIE show brush formation, i.e. the vibration at 1119cm^{-1} shows much higher intensity than that at 1147cm^{-1}. The same finding holds for the pattern formed on a gold surface with MHD islands after 60s RIE. In contrast however, the PEG film formed on a gold substrate previously coated with MHD and etched only for 30s by means of RIE clearly exhibits coil-formation of the PEG layer. This indicates, that after 30s of etching via RIE, the MHD is not completely removed from the gold surface, thus inhibiting the formation of a densely packed PEG film.

These findings are further corroborated by the XPS analysis. Figure 4 displays the C1s and O1s regions of a sputtered gold surface, a MHD-coated gold surface, a PEG-coated gold surface after MHD adsorption and removal via 60s RIE treatment, and a patterned sample also etched for 60s (same samples as displayed in Figure 3).

The C1s region reveals the different chemical shifts of aliphatic and carboxylic species. The MHD shows mainly an aliphatic signal, while the non-patterned PEG film exhibits a strong ether peak. The patterned sample, however, shows a clearly observable aliphatic shoulder in the ether peak, indicating the proper formation of the PEG/MHD pattern.

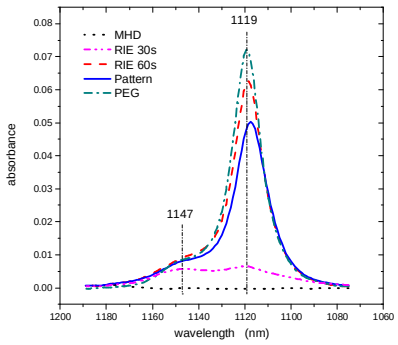

Figure 3: IRRA spectra of the C-O-C backbone vibration of the PEG used as protein-resistant matrix for different surface treatments. MHD- and PEG-coated gold surfaces serve as controls. Further, the efficiency of RIE removal of the MHD was proven by exposing MHD-coated gold surfaces to the RIE treatment for 30s and 60s, respectively, and subsequent PEG adsorption. Finally, a spectrum of a MHD/PEG pattern is displayed.

In the O1s region, the carboxyl group of the MHD shows the two peaks for CO single and double bond, respectively. The positions, which were obtained by a linear background subtraction followed by fitting two Voigt peaks to the data, are in line with their literature values.[6] The same holds for the O1s ether peak of the PEG at 532.9eV.[7] The slight decrease in intensity in the ether peak of the PEG/MHD pattern as compared to the non-patterned PEG film formed on the gold after 60s RIE underlines the success of the nanopatterning process. This intensity drop in the O1s signal can be easily used for calculation of the MHD surface fraction χ_{MHD} by means of the following relation:

$$\chi_{MHD} = \frac{I^0_{PEG} - I_{PEG}}{I^0_{PEG} - I_{MHD}} \quad ,$$

where I^0_{PEG} is the intensity of the ether peak on the non-patterned PEG sample, I_{PEG} its intensity on the patterned PEG/MHD sample, and I_{MHD} that of the MHD reference sample. For determination of the intensities, the spectra were corrected by means of a linear background subtraction and subsequent fitting of Voigt profiles. Thereby, we obtained χ_{MHD} = 9.3% in excellent agreement with the previously estimated value of 8.8%. The experimentally determined value is in line with an average patch diameter of 206.2nm compared to our estimate of

200nm on basis of Figure 2c, assuming random-close packing of the colloidal particles.

Summarizing, the results of the surface analysis on the fabricated nanopatterns confirm the high quality of the patterns and accordingly the feasibility of this approach.

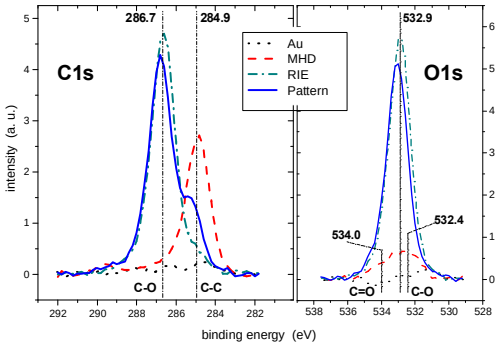

Figure 4: XPS analysis of MHD, PEG, and PEG/MHD-coated gold films as well as a sputtered gold surface used as reference. Shown are the detailed scans of the C1s and O1s regions.

As one interesting application of the method presented here, we nanopatterned gold-coated Biacore sensor chips with the patterns described above. To achieve utmost reproducibility, the sensor chips were processed under the same conditions or even in the same run as the samples used for the surface analysis studies.

Then, the sensor chips were docked to the Biacore X system and used for the antigen/antibody binding studies described above. Figure 5 displays the resulting sensorgrams for subsequent antibody immobilization, BSA passivation, and antigen-binding, respectively, for three different surfaces: one PEG-coated, one MHD-coated sensor, and one PEG/MHD patterned sensor chip. Obviously, the chip fully functionalized with PEG does not show any adsorption at all, thereby confirming the excellent protein resistance of PEG-derivatives.[8] In constrast, the MHD-terminated surface exhibits a significant response to immobilization of the anti-mouse Ab. Despite of that, BSA adsorbs on this surface in the second step, thereby potentially displacing weakly bound Ab molecules. Nevertheless, even after BSA passivation, the surface bears a significant amount of active anti-mouse Ab, as can be seen from binding of the mouse Ab in the third and last step of the sequence. The PEG/MHD patterned surface shows an interesting behavior. While it adsorbs about 37.5% anti-mouse Ab as compared to the MHD-chip in the first step, it exhibits only a weak response to the exposure to BSA of 8.6% as compared to the MHD. In the last step, however, it adsorbs about 35% of the mouse-Ab. While the BSA adsorption of 8.6% matches the experimentally determined surface fraction of MHD of 9.3% very nicely, the antibodies adsorb to an unexpectedly high amount. The reason for this different behavior is probably that in our experiment the antibody adsorption is diffusion-limited due to the low molarity used. Therefore, the patches on the patterned substrate may collect more molecules from the solution in the same time as a corresponding area on the non-patterned surface, which competes with its direct neighborship. The BSA, on the other hand, adsorbs mainly on defect sites of the MHD-coated surface, which have the same density on patterned as well as non-patterned surfaces. Therefore, it reflects simply the surface fraction of the MHD in the respective case.

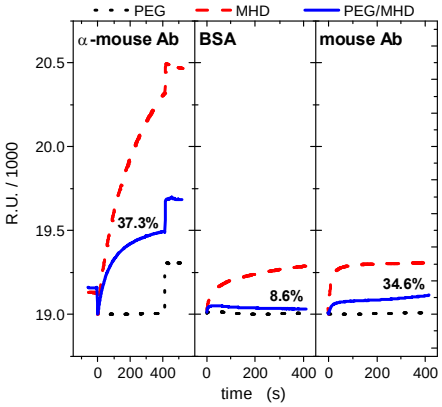

Figure 5: Subsequent antibody, BSA, and antigen adsorption onto a MHD-coated, a PEG-coated, as well as a PEG/MHD patterned Biacore sensor chip, respectively.

4 CONCLUSIONS

We have demonstrated a feasible approach for the fabrication of large-scale nanopatterns formed on continuous gold films, thereby allowing for their analysis by means of several surface-analytical techniques as well as for their application to in-situ biosensing by means of SPR. Under the experimental conditions used, Ab/Ag adsorption seems to be diffusion-limited, with indications for possibility of higher Ab surface density on the patterns. Further experiments for direct determination of the Ab density on the Biacore sensor chips by means of microscopic XPS are currently under way.

ACKNOWLEDGMENT

The authors thank Dr. Y. Ashihara for his continuous support, Drs. H. Takei, M. Isomura, and T. Tanimoto for helpful discussions, and S. Akabane of the Tokyo University of Technology for his assistance with the XPS system. A part of this work was conducted at the AIST Nano-Processing Facility, supported by the Ministry of Education, Culture, Sports, Science and Technology, Japan.

[1] S. V. Rao et al., Mikrochim. Acta, 128, 127, 1998
[2] S. Chen et al., Langmuir, 19, 2859, 2003
[3] A. Valsesia et al., Langmuir, 22, 1763, 2006
[4] Himmelhaus & Takei, Phys. Chem. Chem. Phys., 4, 496, 2002
[5] S. Tokumitsu et al., Langmuir, 2002, 18, 8862
[6] D. A. Hutt & G. J. Leggett, Langmuir 1997, 13, 2740
[7] G. L. Kenausis et al., J. Phys. Chem. B, 2000, 104, 3298
[8] B. Zhu et al., J. Biomed. Mater. Res. 2001, 56, 406